

# Chapter 38

## Investigation of Electrochemical Micromachining Process Using Ultrasonic Heated Electrolyte



M. Soundarrajan  and R. Thanigaivelan 

**Abstract** Electrochemical micromachining (EMM) is one of the important machining methods for fabrication of micro-components on alloys and composites materials. Fabrication of micro hole is the important micro-machined feature, which are used in many components that find application in various fields such as aerospace, automobile, power circuit board (PCB), Ink jet nozzle, and the electronics industries. In this research, micro-hole is generated on 300  $\mu\text{m}$  thick copper workpiece using 460  $\mu\text{m}$  diameter stainless steel electrode. Sodium nitrate ( $\text{NaNO}_3$ ) is considered as electrolyte and during machining process, the electrolyte is heated using Ultrasonic Vibration (USV). The experiments are planned according to  $L_{18}$  Orthogonal Array (OA) using the machining parameters such as electrolyte concentration, machining voltage, duty cycle, and electrolyte temperature. The machining parameters are optimized using Multi-Objective Optimization of Ratio Analysis (MOORA) method. Weight of each response is calculated using entropy method as  $w_j$  for Material Removal Rate ( $\text{MRR}$ ) = 0.4941 and  $w_j$  for Overcut (OC) = 0.5051. The optimal combination obtained using MOORA is 30 g/l of electrolyte concentration, 9 V of machining voltage, 55% of duty cycle, and 36° of electrolyte temperature. According to Analysis of Variance (ANOVA) results, the machining voltage contributes about 55% of overall performance. Additionally, Scanning Electron Microscope (SEM) images are taken for the further understanding of micro-hole profile.

**Keywords** Electrochemical · Heated electrolyte · Ultrasonic · Entropy · MOORA

---

M. Soundarrajan (✉)

Department of Mechanical Engineering, Muthayammal Engineering College (Autonomous), Rasipuram, Namakkal (Dt) 637408, India  
e-mail: [soundarrajan05@gmail.com](mailto:soundarrajan05@gmail.com)

R. Thanigaivelan

Department of Mechanical Engineering, Muthayammal Engineering College (Autonomous), Rasipuram, Namakkal (Dt) 637408, India  
e-mail: [tvelan10@gmail.com](mailto:tvelan10@gmail.com)

© Springer Nature Singapore Pte Ltd. 2019

M. S. Shunmugam and M. Kanthababu (eds.), *Advances in Micro and Nano Manufacturing and Surface Engineering*, Lecture Notes on Multidisciplinary Industrial Engineering, [https://doi.org/10.1007/978-981-32-9425-7\\_38](https://doi.org/10.1007/978-981-32-9425-7_38)

423

## 38.1 Introduction

Due the operational method of traditional machining, manufacturing of burr-free surface in the copper material is the difficult task due to the geometry of the tool, rotational speed, and vibration [1]. EMM is one of the dependable methods for micro-machining of copper with accuracy [2]. In the last decade, various research works has been carried out worldwide to improve the machining performance of EMM. Bhattacharyya et al. [3] have studied the machining performance of EMM on a copper plate in addition to vibration of the tool. They found that sludge removal from the machining zone significantly improved the machining rate and accuracy. Liu et al. [4] have used two types of electrolytes such as aqueous NaCl and ethylene glycol mixed NaCl in EMM on titanium alloy. These electrolytes significantly influence the taper angle and surface roughness. Zhang et al. [5] have used as quasi-solid electrolyte (agarose hydrogel) in NaOH solution to fabricate the micro-tools in EMM. They noted that the accuracy of micro-tool increased significantly in quasi-solid electrolyte than the liquid electrolyte. Guodong et al. [6] have investigated the effect composite electrolyte at different concentration levels for machining stainless steel. They found that the mixture of sodium nitrate with sodium citrate stimulates the ion attraction in the electrolyte. Therefore, disposal of dissolved material is unhindered in the inter-electrode gap which leads to high material removal and better accuracy. Sekar et al. [7] have blended the nanocopper particles in aqueous NaCl electrolyte to machine high carbon and high chromium die steel. The copper particle crashes the hydrogen bubbles in the machining area resulting in an increase in the material removal rate and good surface quality. The optimization of process parameters plays a vital role in manufacturing for reducing the machining time and cost. Therefore, various optimization techniques has been followed by the researchers since the last decade. Jeykrishnan et al. [8] have used the Taguchi technique in ECM on D3 die steel to optimize the machining parameters. From the above literatures, it is understood that the researchers have improved the EMM performance with various types of electrolytes and optimized the process parameters with different techniques. This research focuses on electrolyte heating and in electrochemical machining, the electrolyte temperature plays a significant role in material removal [9]. Different methods are adapted by the researchers to heat the electrolyte and all those methods have disadvantages of heating the subsystems of the EMM setup. Considering this difficulty, a detailed experiment is planned to introduce USV to simultaneously heat and vibrate the electrolyte [10]. Here the USV is kept in the electrolyte tank and heating of the other EMM subsystems is averted. The effect of electrolyte temperature on EMM process is studied with  $L_{18}$  OA experiment design and the process parameters are optimized by the MOORA method.

## 38.2 Experimental Method

Figure 38.1 shows the EMM system used for conducting experiments. The experiments are carried out using an indigenously developed system. The EMM system operated with the subsystems such as tool feeding system, pulse rectifier, and electrolyte supply system. Stainless steel of  $\Phi$  460  $\mu\text{m}$  is used as electrode, and 300  $\mu\text{m}$  thick copper plate is used as a work-piece. The electrode is insulated with epoxy resin to reduce overcut. The aqueous sodium nitrate ( $\text{NaNO}_3$ ) is used as an electrolyte. The machining time has been noted using a stop watch for through-hole machining. The completion of through hole is witnessed by evaluation of hydrogen gas bubbles beneath the workpiece. The experiments are carried out on the basis of  $L_{18}$  OA and the temperature of the electrolyte is measured using a digital thermometer. Commercially available 24 V ultrasonic mist maker is used as the ultrasonic vibrator, which is fixed in the electrolyte tank in a partially submerged position. The ultrasonic vibrator inbuilt with 110 kHz piezoelectric transducer and  $\Phi$  20 mm ceramic plate to generate high-frequency vibration is passed beneath the electrolyte surface. The high-frequency vibration creates rapid collision among the water molecules; consequently, the kinetic energy of the water molecules increases; due to this, the electrolyte heat increases in the machining zone (Fig. 38.2).

The machining parameters are varied for different levels during the experiments and MRR and OC are evaluated for the assessment of the machining performance. From the preliminary study, the machining parameters and their levels are fixed as shown in Table 38.1. The variable machining time and hole diameter of each experiment have been displayed in Table 38.2. The MRR has been evaluated by the ratio of constant thickness of work material in  $\mu\text{m}$  to the variable machining time in seconds and the difference between the tool and hole diameter is considered for OC in  $\mu\text{m}$ . Optical microscope image is used for the evaluation of hole diameter [11].

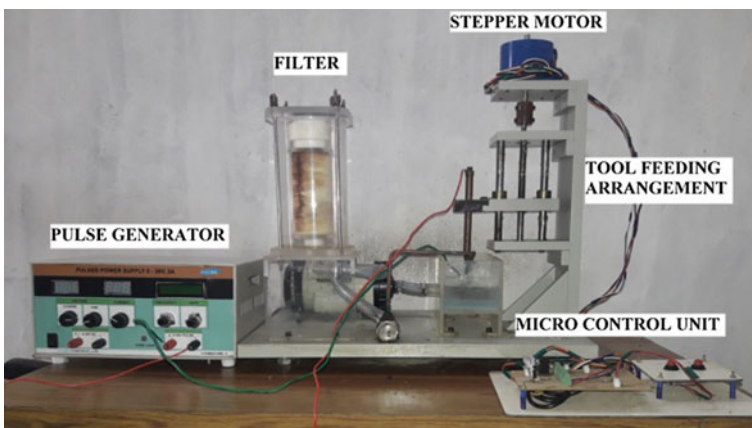


Fig. 38.1 EMM system

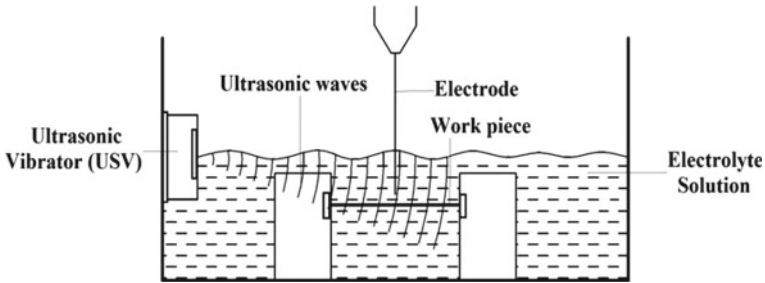


Fig. 38.2 Electrolyte tank attached with ultrasonic vibrator

Table 38.1 Machining parameters and their levels

Symbol	Factors	Level 1	Level 2	Level 3
EC	Electrolyte concentration (g/l)	20	25	30
MV	Machining voltage (V)	7	8	9
DC	Duty cycle (%)	45	55	65
ET	Electrolyte temperature (°C)	32	34	36

Machining parameters and their responses are shown in Table 38.2, which are considered to evaluate the optimal combination using entropy-weighted MOORA method.

### 38.3 MOORA (Multi-objective Optimization on the Basis of Ratio Analysis) Optimization Method

MOORA is one of best and simple tools to find the optimal parametric combination from the experiment results. The following steps are followed for the ranking [12].

Step 1: The decision matrix consist of ‘n’ attributes and ‘m’ alternatives and the responses are kept in the matrix as shown in the Eq. 38.1.

$$Y = \begin{bmatrix} y_{11} & y_{12} & y_{13} & \dots & \dots & y_{1n} \\ y_{21} & y_{22} & y_{23} & \dots & \dots & y_{2n} \\ y_{31} & y_{32} & y_{33} & \dots & \dots & y_{3n} \\ \vdots & \vdots & \vdots & \ddots & \ddots & \vdots \\ \vdots & \vdots & \vdots & \ddots & \ddots & \vdots \\ y_{m1} & y_{m2} & y_{m3} & \dots & \dots & y_{mn} \end{bmatrix} \tag{38.1}$$

Step 2: The matrix responses are normalized using Eq. 38.2.

**Table 38.2** L<sub>18</sub> OA and their responses with MOORA rank

Ex. no	EC (g/l)	MV (V)	DC (%)	ET (°C)	Machining time (s)	Hole dia (μm)	MRR (μm/s)	OC (μm)	MOORA value (Y <sub>i</sub> )	Rank
1	20	7	55	32	986.84	565.60	0.304	105.6	0.0514	18
2	20	8	45	34	582.52	563.22	0.515	103.22	0.0871	15
3	20	9	65	36	432.90	604.02	0.693	144.02	0.1171	3
4	25	7	55	34	568.18	596.82	0.528	136.82	0.0892	13
5	25	8	45	36	391.13	547.61	0.767	87.61	0.1032	8
6	25	9	65	32	360.14	539.21	0.833	79.21	0.0933	10
7	30	7	45	32	552.49	564.41	0.543	104.41	0.0918	11
8	30	8	65	34	412.09	558.41	0.728	98.41	0.1159	4
9	30	9	55	36	321.54	562.01	0.933	102.01	0.1202	1
10	20	7	65	36	657.89	530.81	0.456	70.81	0.0770	16
11	20	8	55	32	391.13	548.80	0.767	88.8	0.1046	7
12	20	9	45	34	342.08	546.40	0.877	86.4	0.1018	9
13	25	7	45	36	704.23	539.21	0.426	79.21	0.0720	17
14	25	8	65	32	562.85	584.82	0.533	124.82	0.0902	12
15	25	9	55	34	356.29	551.21	0.842	91.21	0.1075	6
16	30	7	65	34	574.71	553.61	0.522	93.61	0.0883	14
17	30	8	55	36	431.03	561.62	0.696	101.62	0.1176	2
18	30	9	45	32	307.38	552.41	0.976	92.41	0.1089	5

$$k_{ij} = \frac{y_{ij}}{\sqrt{\sum_{i=1}^m y_{ij}^2}} \quad j = 1, 2, \dots, n \quad (38.2)$$

where  $k_{ij}$  is a dimension-less number which belongs to the interval [0, 1] for  $i$ th alternative and  $j$ th attribute which represents the normalized performance.

Step 3: The maximum normalized performance values are should added (for beneficial attributes) and minimum normalized values are should subtracted (non-beneficial attributes) as in Eq. 38.3

$$q_i = \sum_{j=1}^g k_{ij} - \sum_{j=g+1}^n k_{ij} \quad (38.3)$$

where  $g$  is the no. of attributes to be maximized,  $(n - g)$  is the number of attributes to be minimized, and  $q_i$  is the normalized assessment value.

Step 4: The importance of responses to the attributes  $w_j$  are be multiplied with the corresponding weight.

$$q_i = \sum_{j=1}^g w_j k_{ij} - \sum_{j=g+1}^n w_j k_{ij} \quad (j = 1, 2, \dots, n) \quad (38.4)$$

where  $w_j$  is the weighted value obtained using the entropy method. Then these  $q_i$  values are ranked as per the preference values, in which higher value deserves the optimal combination.

## 38.4 Result and Discussion

### 38.4.1 Input Parameters Effect on MRR

The machining parameters and their mean responses are plotted in the graph as depicted in Figs. 38.3, 38.4, 38.5, and 38.6. It is evident from the figures that higher parameter level deserves the higher MRR. The ultrasonic vibration heats the electrolyte by creating the molecular collision. Due to heating, the ions in the electrolyte experience higher displacement, resulting in higher MRR [13]. Additionally, the USV dispels the debris produced during machining from the machining zone. This continues the removal of debris that helps to improve the machining, resulting in higher MRR.

**Fig. 38.3** EC versus MRR and OC

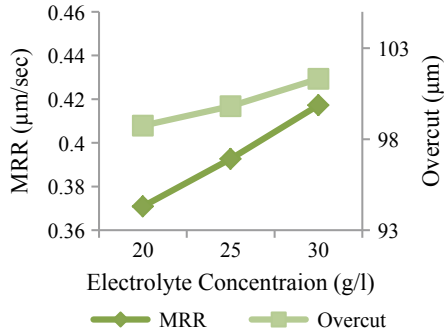


**Fig. 38.4** MV versus MRR and OC

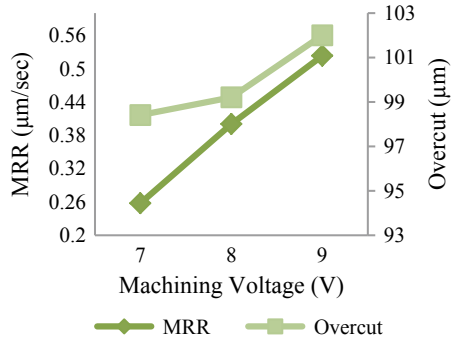
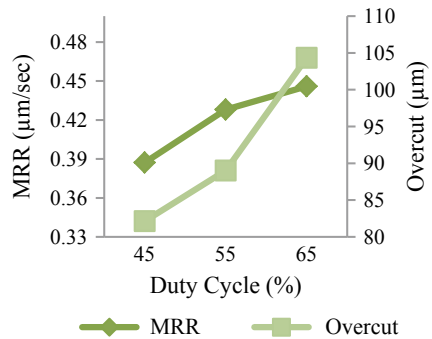


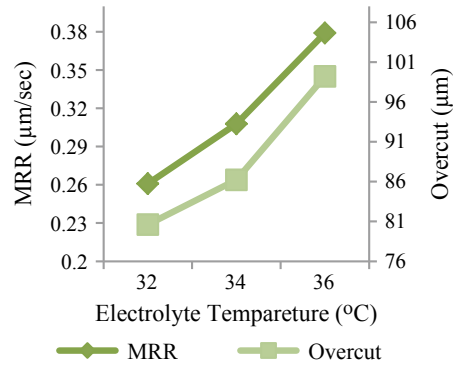
**Fig. 38.5** DC versus MRR and OC



### 38.4.2 Input Parameters Effect on OC

The USV-heated electrolyte produces the overcut ranging from 75 to 110  $\mu\text{m}$ . This range is comparatively lesser with the existing literatures [9]. USV electrolyte contributes for two times better overcut compared to the other electrolyte heating technique. The use of USV removes the debris continuously and possibilities of stray

**Fig. 38.6** ET versus MRR and OC



attack are reduced. The responses against the machining parameters are displayed in Figs. 38.3, 38.4, 38.5, and 38.6.

### 38.4.3 MOORA

Entropy-weighted MOORA method has been adopted for the optimization of MRR and OC using USV-heated electrolyte. Equations 38.1–38.4 are used for the MOORA values and its ranking, which is indexed in Table 38.2. The attribute weights are assigned using the entropy method as  $w_j = 0.4941$  for MRR and  $w_j = 0.5051$  for OC. The highest MOORA value is considered as the best value, which holds the first rank and considered as the optimal combination for the best machining performance. Therefore, experimental run 9 holds the highest MOORA value 0.1202. The experimental run 9 shows better result—0.933  $\mu\text{m/s}$  MRR and 102.01  $\mu\text{m}$  OC—compared to other experimental runs using MOORA. Also, the experimental runs 17 (0.1176) and 3 (0.1171) are the next two optimal combinations. Therefore, 30 g/l of electrolyte concentration, 9 V of machining voltage, 55% duty cycle, and 36° of electrolyte temperature are recommended for better machining performance.

### 38.4.4 ANOVA Table for MOORA

MOORA values are statically studied by ANOVA which identifies the significant process parameters and its contribution toward the machining performance. Therefore, machining voltage contributes about 55.51% in machining performance. Table 38.3 shows the percentage contribution of electrolyte concentration and temperature as 18.78% and 7.28%, respectively. According to ANOVA Table 38.3, duty cycle is insignificant compared to other parameters.



**Table 38.3** ANOVA table for MOORA

Symbol	DF	Seq SS	Adj MS	F	% of contribution
EC	2	0.0010356	0.0005178	4.86	18.78
MV	2	0.0030605	0.0015302	14.3	55.51
DC	2	0.0000572	0.0000286	0.27	1.04
ET	2	0.0004013	0.0002006	1.88	7.28
Error	9	0.0009588	0.0001065		17.39
Total	17	0.0055133	0.015		100

### 38.5 SEM Analysis

SEM graphs that are shown in Figs. 38.7 and 38.8 are for the first and second optimal combinations. Figure 38.7 shows the round circumference micro-hole without any irregularity in major areas. Although one side of its circumference had an over-etched surface, the profile of the micro-hole is circular without any irregularities. It is due to the fact that the ultrasonic vibrations passed beneath the electrolyte from one side of tank and the smaller tank capacity makes way for debris encounter resulting in

**Fig. 38.7** SEM for the first optimal solution (30 g/l, 9 V, 55%, 36 °C)

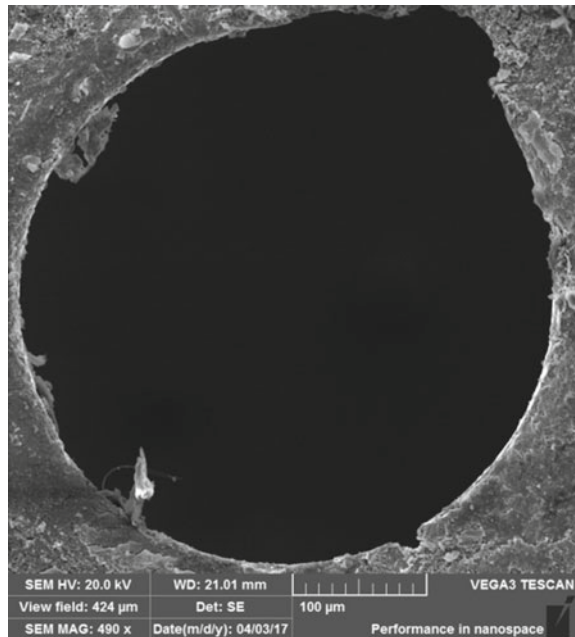
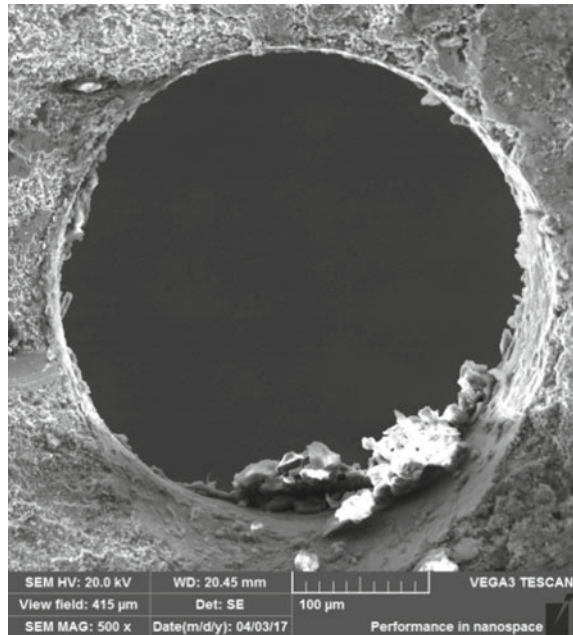


**Fig. 38.8** SEM for the second optimal solution (30 g/l, 8 V, 55%, 36 °C)



few stray cuts. Figure 38.8 shows the better circularity, machined under the second optimal combination.

### 38.6 Conclusion

EMM performance is enhanced with aids of USV heated electrolyte. The experiments is planned based on the  $L_{18}$  OA. Entropy method is used to identify the weight of each response. MOORA method has been used to calculate the optimal combination.

- Weight for each responses are calculated using as  $w_j$  for  $MRR = 0.4941$  and  $w_j$  for  $OC = 05051$  using entropy method.
- The optimal combinations for better performance are 30 g/l of electrolyte concentration, 9 V of machining voltage, 55% duty cycle, and 36° of electrolyte temperature.
- Based on ANOVA, the machining voltage contributes about 55% in the overall machining performance.
- USV-heated electrolyte shows two times lesser overcut compared to the other methods.

- USV heated electrolyte is more suitable for better MRR and accuracy. Further experiments can be planned to hinder the over-etching surface in the machining area.

**Acknowledgements** The authors thank the Government College of Engineering, Salem, for providing the SEM facilities. The authors thank the management of Muthayammal Engineering College, Rasipuram, Tamil Nadu, for the encouragement and support. The authors are grateful to the management of Sona College of Technology, Salem, for providing the optical microscope facilities to verify the overcut.

## References

1. Venkatesh, V., Swain, N., Srinivas, G., Kumar, P., Barshilia, H.C.: Review on the machining characteristics and research prospects of conventional micro-scale machining operations. *Mater. Manuf. Process.* **32**(3), 1042–6914 (2017). <https://doi.org/10.1080/10426914.2016.1151045>
2. Anasane, S.S., Bhattacharyya, B.: Electrochemical micromachining of titanium and its alloys. In: Kibria, G., Bhattacharyya, B., Davim, J. (eds.) *Non-traditional Micromachining Processes. Materials Forming, Machining and Tribology*. Springer, Cham (2017)
3. Bhattacharyya, B., Malapati, M., Munda, J.: Influence of tool vibration on machining performance in electrochemical micro-machining of copper. *Int. J. Mach. Tools Manuf.* **47**(2), 35–342 (2007). <https://doi.org/10.1016/j.ijmactools.2006.03.005>
4. Liu, W., Zhang, H., Luo, Z., Zhao, C., Ao, S., Gao, F., Sun, Y.: Electrochemical micromachining on titanium using the NaCl-containing ethylene glycol electrolyte. *J. Mater. Process. Technol.* **255**, 784–794 (2018). <https://doi.org/10.1016/j.jmatprotec.2018.01.009>
5. Zhang, H., Ao, S., Liu, W., Luo, Z., Niu, W., Guo, K.: Electrochemical micro-machining of high aspect ratio micro-tools using quasi-solid electrolyte. *Int. J. Adv. Manuf. Technol.* **91**(9–12), 2965–2973 (2017). <https://doi.org/10.1007/s00170-016-9900-x>
6. Guodong, L., Yong, L., Quancuna, K.: Selection and optimization of electrolyte for micro electrochemical machining on stainless steel 304. *Procedia CIRP* **42**, 412–417 (2016). <https://doi.org/10.1016/j.procir.2016.02.223>
7. Sekar, T., Arularasu, M., Sathiyamoorthy, V.: Investigations on the effects of nano-fluid in ECM of die steel. *Measurement* **83**, 38–43 (2016). <https://doi.org/10.1016/j.measurement.2016.01.035>
8. Jeykrishnan, J., Vijaya Ramnath, B.: Optimization of process parameters in electro-chemical machining (ECM) of D3 die steels using Taguchi technique. *Mater. Today Proc.* **4**(8), 7884–7891 (2017). <https://doi.org/10.1016/j.matpr.2017.07.124>
9. Thanigaivelan, R., Arunachalam, R.M., Kumar, M.: Performance of electrochemical micromachining of copper through infrared heated electrolyte. *Mater. Manuf. Process.* **33**(4), 383–389 (2018). <https://doi.org/10.1080/10426914.2017.1279304>
10. Yaralioglu, G.: Ultrasonic heating and temperature measurement in microfluidic channels. *Sens. Actuators A Phys.* **170** (1–2), 1–7 (2011). <https://doi.org/10.1016/j.sna.2011.05.012>
11. Soundarrajan, M., Thanigaivelan, R.: Intervening variables in electrochemical micro machining for copper. In: *International Conference on Precision, Meso, Micro and Nano Engineering (COPEN 10)*, Indian Institute of Technology Madras, Chennai, India (2017)

12. Chakraborty, S.: Application of the MOORA method for decision making in manufacturing environment. *Int. J. Adv. Manuf. Technol.* **54** (9–12), 1155–1166 (2011). <https://doi.org/10.1007/s00170-010-2972-0>
13. Van Deconinck, D., Damme, S., Deconinck, J.: A temperature dependent multi-ion model for time accurate numerical simulation of the electrochemical machining process. Part II: Numerical simulation. *Electrochimica Acta* **69**, 120–127 (2012). <https://doi.org/10.1016/j.electacta.2012.02.079>